HYPERSPECTRAL UNMIXING BY REWEIGHTED LOW RANK AND TOTAL VARIATION

Rui Wang[a,b], Wenzhi Liao[a], Heng-Chao Li[b], Hongyan Zhang[a,c], Aleksandra Pižurica[a]

[a] Ghent University, TELIN-IPI-iMinds, Sint-Pietersnieuwstraat 41, B-9000 Ghent, Belgium
[b] Sichuan Provincial Key Laboratory of Information Coding and Transmission, Southwest Jiaotong University, Chengdu 610031, China
[c] State Key Lab. of Inf. Eng. in Surveying, Mapping and Remote Sensing, Wuhan University, China
Email: wangruinew@163.com, wliao@telin.ugent.be

ABSTRACT

In recent years, sparse regression has drawn much attention in hyperspectral unmixing. The well known *sparse unmixing via variable splitting augmented Lagrangian* (SUnSAL) and *sparse unmixing via variable splitting augmented Lagrangian and total variation* (SUnSAl-TV) aim to find the sparsest abundance of every data vector individually. However, these methods ignore the global structure of all the vectors. In this paper, we propose a novel hyperspectral unmixing method by exploiting low rank property of the abundance matrix. Our proposed method find the lowest-rank representation of a collection of the abundance vectors by using reweighted low rank constraint. This way, our proposed unmixing method better captures the global structure of the abundance matrix and improve the accuracy of abundance estimation. Our approach also takes the spatial context into account by a TV constraint. Experimental results on both the synthetic and real hyperspectral data demonstrate the effectiveness of our proposed algorithm.

***Index Terms*—** Hyperspectral remote sensing, unmixing, low rank, reweighted

1. INTRODUCTION

Due to the low spatial resolution of the sensor, mixed pixels are often encountered in hyperspectral imagery (HSI). To some extent, the existence of mixed pixels restricts the exploitation, processing, and applications of HSI in practice. Thus, spectral unmixing is an important technique for hyperspectral data exploitation, which decomposes a mixed pixel into a collection of constituent materials (also called endmembers) and their relative proportions (also called abundances) [1].

In the past few years, many methods have been proposed for hyperspctral unmixing. Linear mixing models (LMM) assume that the spectrum of each pixel can be approximately represented by a linear mixture of endmember spectra weighted by the corresponding fractional abundances [2]. The geometrical and statistical frameworks [2] are two of widely used methods for hyperspectral unmixing. However, they generally require the presence of pure materials and the estimation of the number of endmembers in a given scene. Sparse unmixing [3], as a semisupervised approach for linear spectral unmixing, has been approached in recent years. In sparse unmixing method, we try to find the optimal subset of signatures in a (potentially very large) spectral library that can best model each mixed pixel in the scene. Although sparse unmixing techniques have shown obvious benefits, they are limited by the high correlation of spectral libraries. *Sparse unmixing via variable splitting augmented Lagrangian and total variation* (SUnSAL-TV) [4] sidesteps the limitations of sparse unmixing by taking spatial information of the given scene into account. However, l_1 norm aims to find out the sparsest representation of each vector individually without any global constaint on its solution. This will lead to poor unmixing performances, especially for observed HSI degraded by noise.

In this paper, we propose a new method for hyperspectral unmixing by reweighted low rank and total variation (HURLR-TV). Typical abundance matrices are both low rank and spase. Here we model the sparsity of the abundance in the domain of finite differences by imposing a TV regularizer as in [4]. This way we take into account the spatial smoothness properties of the abundance entries too. In constrast to [4], where the TV regularizer was combined with the l_1 norm, we employ the low-rank model. Extensive experiments on both synthetic and real hyperspectral data were conducted, and the results show clear advantages of the proposed algorithm over some other hyperspectral unmixing approaches. The rest of this paper is organized as follows: Section 2 briefly describes low rank representation. Section 3 details the proposed method. Our experimental results with simulated and real hyperspectral data sets are described in Section 4. Section 5 concludes this paper.

This work was supported by China Scholarship Council, the FWO project G037115N: Data fusion for image analysis in remote sensing and the National Natural Science Foundation of China under Grant 61371165.

2. BACKGROUND

2.1. Low-Rank Representation

Low rank is an important characteristic in image, which is widely used in image restoration [5], texture characterization [6], hyperspectral image processing [7] and many other applications. Consider a set of data vectors $\mathbf{Y} = [\mathbf{y}_1, \mathbf{y}_2, ..., \mathbf{y}_N] \in \mathbb{R}^{L\times N}$, which can be represented by a linear transformation of a dictionary $\mathbf{A} \in \mathbb{R}^{L\times p}$:

$$\mathbf{Y} = \mathbf{AX} + \mathbf{N} \tag{1}$$

where $\mathbf{X} = [\mathbf{x}_1, \mathbf{x}_2, ..., \mathbf{x}_N] \in \mathbb{R}^{p\times N}$ is the coefficient matrix with each $\mathbf{x}_i$ being the representation of $\mathbf{y}_i$. The use of a low rank assumption leads to solving the follwing problem

$$\min_{\mathbf{X}} rank(\mathbf{X}) \qquad \text{subject to} \quad \mathbf{AX} = \mathbf{Y}. \tag{2}$$

where the optimal solution $\mathbf{X}^*$ is the lowest rank representation of data $\mathbf{Y}$. The resulting optimization problem is difficult to solve, hence, it is typically relaxed such that it admits convex optimization, as follows [9]

$$\min_{\mathbf{X}} \|\mathbf{X}\|_* \qquad \text{subject to} \quad \mathbf{AX} = \mathbf{Y} \tag{3}$$

where $\|\mathbf{X}\|_* = \sum_i \sigma_i$ denotes the nuclear norm [10] of $\mathbf{X}$ and σ_i is a singular value of $\mathbf{X}$.

3. PROPOSED APPROACH

In this paper, we develop a new hyperspectral unmixing method called *hyperspectral unmixing via reweighted low rank and total variation* (HURLR-TV). Low rankness treats all the vectors together, thus better captures the global structure of the recovered abundance matrix. Inspired by the success of weighted l_1 minimization [11], we use weighted low rank regularizer to improve the low rank of the abundance matrix. Our method based on reweighted low rank and the spatial regularizer sovles the following optimization problem

$$\begin{aligned} &\min_{\mathbf{X}} \frac{1}{2}\|\mathbf{Y} - \mathbf{AX}\|_F^2 + \lambda \sum_i w_i\sigma_i + \lambda_{TV} TV(\mathbf{X}) \\ &\text{subject to } \ \mathbf{X} \geq 0 \end{aligned} \tag{4}$$

where $\mathbf{Y} \in \mathbb{R}^{L\times N}$, $\mathbf{A} \in \mathbb{R}^{L\times p}$, $\mathbf{X} \in \mathbb{R}^{p\times N}$ are the observed data, spectral library and abundance matrix, respectively. σ_i is the singular value of the abundance matrix $\mathbf{X}$, the w_i is the weight of singular value for singular value σ_i

$$w_i^{(t+1)} = \frac{1}{\sigma_i^{(t)} + \varepsilon} \tag{5}$$

The rank of the abundance matrix is actually the number of nonzero singular values of the abundance matrix. We explore large weights to discourage nonzero singular values and small weights to encourage nonzero singular values. The reweighted low rank promotes the low rank of the abundance matrix and captures the global structure better. The TV regularizer penalizes the differences between the vectors in the abundance matrix that correspond to neighboring pixels as in [4]:

$$TV(\mathbf{X}) \equiv \sum_{\{i,j\}\in\varepsilon} \|\mathbf{x}_i - \mathbf{x}_j\|_1 \tag{6}$$

where ε denotes the set of horizontal and vertical neighbors. The problem (4) can be written in the following equivalent form

$$\min_{\mathbf{X}} \frac{1}{2}\|\mathbf{Y} - \mathbf{AX}\|_F^2 + \lambda \sum_i w_i\sigma_i + \lambda_{TV} TV(\mathbf{X}) + \iota_{R+}(\mathbf{X}) \tag{7}$$

where $\iota_{R+}(\mathbf{X}) = \sum_{i=1}^N \iota_{R+}(\mathbf{x}_i)$ is the indicator function ($\mathbf{x}_i$ represents the ith column of $\mathbf{X}$. $\iota_{R+}(\mathbf{x}_i)$ is zero if $\mathbf{x}_i$ belongs to the nonnegative orthant and $+\infty$ otherwise).

We solve (7) by *the alternating direction method of multipliers* (ADMM) method [12].

4. EXPERIMENTAL RESULTS AND DISCUSSIONS

In this section, unmixing experiments are performed on the synthetic and real hyperspectral images. Results of some very recent methods such as *sparse unmixing via variable splitting augmented Lagrangian* (SUnSAL) [3] and SUnSAL-TV [4] are compared to the results of our HURLR-TV method.

The spectral library used in these synthetic image experiments is $\mathbf{A} \in \mathbb{R}^{224\times 240}$, which is generated by randomly selecting 240 different materials from the USGS library [1] . It comprises spectral signatures with reflectance values given in 224 spectral bands and distributed uniformly over the interval $0.4-2.5\mu$m. We simulate the synthetic data cube with 75×75 pixels and 224 bands per pixel based on LMM by using five randomly chosen spectral signatures from the library $\mathbf{A}$ as the endmembers and by generating the abundances following the methodology of [4]. Finally, the simulated hyperspectral data is degraded by Gaussian noise with three different levels of the signal-to-noise ratio, i.e., 20dB, 30dB, and 40dB.

We adopt the signal-to-reconstruction error (SRE) and the probability of success (p_s) as the objective metrics for quantitative evaluation. Specifically, the SRE in dB is defined as $\text{SRE} = 10\log_{10}(E[\|\mathbf{x}\|_2^2]/E[\|\mathbf{x} - \hat{\mathbf{x}}\|_2^2])$ [3], and p_s is given by $p_s = P(\|\hat{\mathbf{x}} - \mathbf{x}\|^2/\|\mathbf{x}\|^2 < 3.16)$, where $\hat{\mathbf{x}}$ is the estimated fractional abundance vector of the true fractional abundance vector $\mathbf{x}$ and $E[\cdot]$ stands for mean value[3]. These metrics indicate the quality of the reconstruction of spectral mixtures. The larger these values are, the better the performance of the algorithm for recovering the abundances are. Table 1 demonstrates the unmixing results of SRE and p_s. Figure 1

[1] http://speclab.cr.usgs.gov/spectral.lib06

shows the abundance maps estimated by different methods for one randomly selected endmember in synthetic data with SNR=20dB.

Table 1. Performance of different unmixing approaches on simulated hyperspectral data

SNR(in dB)	Algorithm	SRE(in dB)	p_s
20	SUnSAL	4.4661	0.3552
	SUnSAL-TV	10.8890	0.9889
	HURLR-TV	**11.9134**	**1**
30	SUnSAL	9.4353	0.9292
	SUnSAL-TV	18.7212	1
	HURLR-TV	**22.0214**	**1**
40	SUnSAL	11.1475	1
	SUnSAL-TV	28.1640	1
	HURLR-TV	**30.0855**	**1**

The results in Table 1 show that HURLR-TV outforms other methods in terms of SRE at different noise levels. In terms of p_s, HURLR-TV and SUnSAL-TV give optimal results, and SUnSAL fails at low-SNR. Fig. 1 demonstrates that the abundance obtained by SUnSAL looks very noisy because the spatial information is not taken into account. By considering the spatial information, the abundances estimated by SUnSAL-TV and HURLR-TV appear very similar visually, but the proposed method retrieves more details (compare the reconstructed squares in the sencond and the third row of Fig. 1(c) and Fig. 1(d)).

The real HSI used in the experiments is a subimage of 250×191 pixels and 188 bands from the publicly available AVIRIS Cuprite data collected in 1997. The Cuprite site is well understood mineralogically, and it has several exposed minerals of interest. The standard spectral library for this data is the USGS library containing 498 pure endmember signatures. Essential calibration was undertaken in order to mitigate the mismatches between the hyperspectral image and the signatures in the library [3]. The estimated results are demonstrated in Fig. 2.

From Fig. 2, we have similar findings: sparse unmixing methods either perform poor on noise reduction (e.g.SUnSAL) or oversmooth the abundance map (e.g.SUnSAL-TV). By exploiting the low rank property and capturing the global structure of the data, our proposed method produces better results.

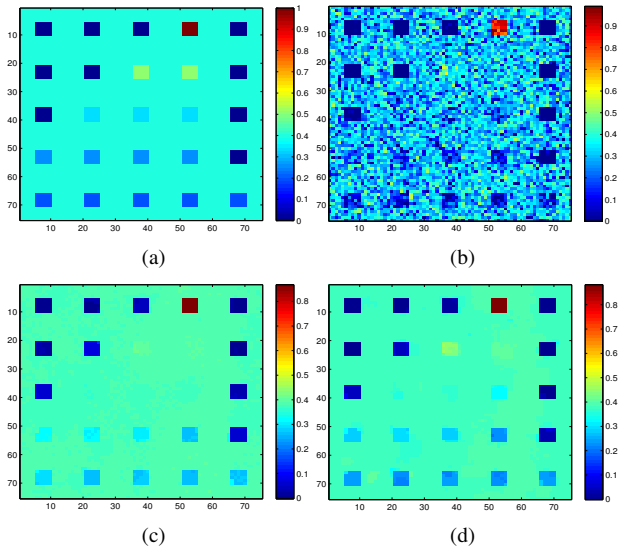

Fig. 1. Abundance maps obtained by different unmixing methods for $5th$ endmembers in the synthetic data with SNR=20dB : (a) Ground truth, (b) SUnSAL, (c) SUnSAL-TV and (d) HURLR-TV.

5. CONCLUSIONS

This paper proposes a novel hyperspectral unmixing method based on reweighted low rank to improve the accuracy of abundance estimation. The reweighted low rank can capture the global structure of the abundance matrix through finding the lowest rank representation of all data jointly. The spatial information is utilized throgh a TV regularizer. Simulated and real hyperspectral data sets are used to test the performance of the proposed HURLR-TV. The experimental results show consistently improvement over the related SUnSAL-TV method.

References

[1] N. Keshava and J. F. Mustard, "Spectral unmixing," *IEEE Signal Process. Mag.*, vol. 19, no. 1, pp. 44-57, 2002.

[2] J. M. Bioucas-Dias, A. Plaza, N. Dobigeon, M. Perente, Q. Du, P. Gader, and J. Chanussot, "Hyperspectral unmixing overview: geometrical statistical, and sparse-regression-based approaches," *IEEE J. Sel. Topics Appl. Earth Observ. Remote Sens.*, vol. 5, no. 2, pp. 354-379, 2012.

[3] M. D. Iordache, J. M. Bioucas-Dias, and A. Plaza, "Sparse unmixing of hyperspectral data," *IEEE Trans. Geosci. Remote Sens.*, vol. 49, no. 6, pp. 2014-2039, 2011.

[4] M. D. Iordache, J. M. Bioucas-Dias, and A. Plaza, "Total variation spatial regularization for sparse hyperspec-

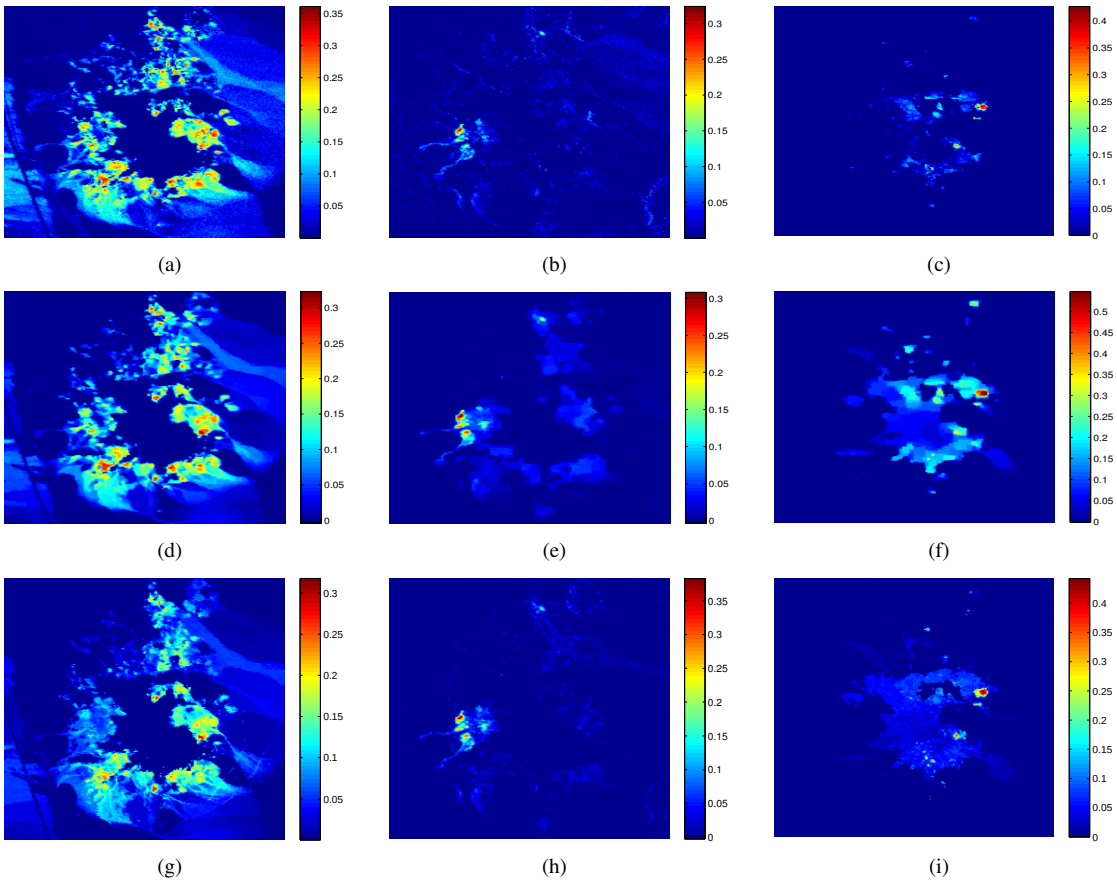

Fig. 2. Fractional abundance maps estimated for the AVIRIS Cuprite subscene with the USGS library. From left to right: Alunite, Buddingtonite, and Chalcedony. (a)-(c) SUnSAL, (d)-(f) SUnSAL-TV, (g)-(i) HURLR-TV.

tral unmixing," *IEEE Trans. Geosci. Remote Sens.*, vol. 50, no. 11, pp. 4484-4502, 2012.

[5] Y. Peng, J. Suo, Q. Dai, S. Member, and W. Xu, "Reweighted low-rank matrix recovery and its application in image restoration," *IEEE Trans. on cybernetics*, vol. 44, no. 12, pp. 2418-2430, 2014.

[6] S. Ono, T.Miyata and I. Yamada, "Cartoon-texture image decomposition using blockwise low-rank texture characterization," *IEEE Trans. Image. Process.*, vol. 23, no. 3, pp. 1128-1142, 2014.

[7] W. He, H. Zhang, L. Zhang, and H. Shen, "Total-variation-regularized low-rank matrix factorization for hyperspectral image restoration," *IEEE Trans. Geosci. Remote Sens.*, vol. 54, no. 1, pp. 178-188, 2016.

[8] G. Liu, Z. Lin, S. Yan, Y. Yu and Y. Ma,"Robust recovery of subspace structures by low-rank respresentation," *IEEE Trans. Pattern Anal. Mach. Interll.*, vol. 35, no. 1, pp. 171-184, 2013.

[9] E. J. Candes, B. Recht, "Exact matrix completion via convex optimization," *Foundations of Computational mathematics*, vol. 9, no. 6, pp. 717-772, 2009.

[10] M. Fazel. "Matrix rank minimization with applications," PhD thesis, Stanford University, 2002.

[11] E. J. Candes, M. B. Wakin, and S. P. Boyd, "Enhancing sparsity by reweighted minimization," *J. Fourier Anal. Appl.*, vol. 14, no. 5-6, pp. 877-905, 2008.

[12] M. V. Afonso, J. M. Bioucas-Dias, and M. A. T. Figueiredo, "An augmented Lagrangian approach to the constrained optimization formulation of imaging inverse problems," *IEEE Trans. Image Process.*, vol. 20, no. 3, pp. 681-695, 2011.